

The paramagnetic spectral response from LiV_2O_4

A P Murani¹, A Krimmel², J R Stewart¹, M Smith³, P Strobel⁴, A Loidl²
and A Ibarra-Palos⁴

¹ Institut Max von Laue Paul Langevin, 6 Rue Jules Horowitz, 38042 Grenoble, France

² Institut für Physik, Universität Augsburg, D-86159 Augsburg, Germany

³ School of Chemistry, University of St Andrews, Fife KY16 9SS, UK

⁴ Laboratoire de Crystallographie, CNRS, BP 166 X, 38042 Grenoble, France

Abstract

At low temperatures LiV_2O_4 exhibits short range paramagnetic correlations, peaked on momentum transfer $Q \sim 0.6 \text{ \AA}^{-1}$. A marked evolution in the spectral intensity towards low Q values ($Q \rightarrow 0$) and low energy transfers ω is observed as the temperature is increased above 2 K (to ~ 10 K and higher). The form of the spectral response is rather complex, requiring *at least* two spectral components to describe the scattering over the relatively small energy range investigated. We show that the observed paramagnetic spin fluctuations in LiV_2O_4 , i.e. the spin degrees of freedom, can account reasonably well for its large specific heat coefficient γ ($=C/T$).

(Some figures in this article are in colour only in the electronic version)

1. Introduction

The compound LiV_2O_4 has aroused considerable experimental and theoretical interest ever since the discovery that it remains paramagnetic down to very low temperatures where it shows a constant susceptibility χ of $\sim 0.01 \text{ cm}^{-3} \text{ mol}^{-1}$ [1, 2], and a large specific heat coefficient γ ($=C/T$) of $\sim 0.42 \text{ J mol}^{-1} \text{ K}^{-2}$, and hence a Wilson ratio R ($\propto \chi/\gamma$) ~ 1.7 [1]. With increasing temperature, the magnetic susceptibility goes through a broad maximum around ~ 16 K [1] and follows the Curie–Weiss behaviour at higher temperatures with a large, but varying, magnitude of the negative intercept increasing with the temperature over which the Curie–Weiss fit is performed [3]. Consequently, the Curie constant also varies with the temperature, yielding a magnetic moment a little larger than expected for localized V^{4+} ions ($g = 2$ and $S = \frac{1}{2}$) for $T < 300$ K. However, a significantly higher moment is obtained over the Curie–Weiss fit range of $600 < T < 1000$ K [3].

The large, negative Curie–Weiss intercept in LiV_2O_4 is attributed to strong antiferromagnetic near-neighbour exchange between the vanadium moments that occupy the octahedral (B) sites in the cubic AB_2O_4 spinel structure and thus form a sublattice consisting of corner-sharing, highly frustrated tetrahedra. A further complexity arises from the fact that

the average number of d electrons per vanadium ion is non-integral, namely 1.5. This has led to a suggestion by Fulde *et al* [4] that the vanadium ions will charge order with half the vanadium ions having one d electron and the other half two d electrons, both species forming interweaving loops and rings. However, a generally accepted picture, supported by band structure calculations [5], is that the ground t_{2g} (cubic) crystal field state is further split by the local trigonal symmetry at the vanadium site into the singlet A_{1g} where one d electron per vanadium is localized and a doublet E_g band which contains the remaining 0.5 d electrons.

In view of these remarkable properties, particularly the large γ and the enhanced, constant χ at low temperatures, LiV_2O_4 has been proclaimed as the first example of a 3d transition metal heavy fermion system, similar to the 4f and 5f heavy fermion systems. A further indication of the heavy fermion character is suggested by the observation of the T^2 variation in the electrical resistivity [6] at low temperatures with a large magnitude of the coefficient A of the T^2 term and the ratio A/γ^2 similar to the values for other heavy fermion systems. However, the electrical resistivity of LiV_2O_4 continues to increase markedly with increasing temperature in contrast with the case for the 4f heavy fermion systems, for example CeAl_3 and UPt_3 , where it saturates out to some small, roughly constant, values [6]. NMR measurements of the inverse relaxation time $1/T_1$ indicate a linear increase from low T up to $>\sim 20$ K reaching a broad maximum followed by a slow decrease beyond ~ 100 K, going through a broad minimum and a gradual increase at higher temperatures [1, 7]. The compound exhibits a number of interesting physical properties that are summarized by Johnston [8].

Neutron inelastic scattering investigations of LiV_2O_4 have been reported by Krimmel *et al* [9] and Lee *et al* [10]. Both groups used polycrystalline samples, since sufficiently large single crystals of LiV_2O_4 necessary for neutron scattering investigations are not yet available. Krimmel *et al* performed time-of-flight measurements using low incident energy neutrons that permitted measurements in neutron energy loss spectroscopy ($\omega > 0$) over an energy range up to ~ 2 meV. They analysed their data taken at constant scattering angles assuming a *single Lorentzian spectral component*. This procedure ignores the variation of intensity with the neutron momentum transfer, Q (directly related to energy transfer ω for fixed scattering angles Θ) and is, therefore, not suitable for a system such as LiV_2O_4 showing strong spin–spin correlations. Also, the rather limited energy range investigated in that experiment, comparable to or smaller than the spectral half-width, hampers a satisfactory analysis of the data, particularly at low temperatures. Lee *et al* used a cold neutron triple-axis spectrometer to obtain data at constant Q but also analysed them using a *single Lorentzian spectral component*. Their data covering a slightly higher energy range up to ~ 3.5 meV also provide some useful insights; however, certain aspects of the spin dynamics have remained unexplored.

In the following we report results of neutron scattering measurements on LiV_2O_4 performed over a larger energy range than in the earlier studies. As found previously, the data at low temperatures show spin correlations peaked on $\sim 0.6 \text{ \AA}^{-1}$ and their strong evolution towards low energies and Q vectors as the temperature is raised. We find that the form of the spectral response is rather complex and that, unlike in previous studies, *more than one (Lorentzian) spectral component* is required to account for the observed scattering. We find also that the observed paramagnetic fluctuations can account for the large specific heat coefficient.

2. Experiment

The present measurements were carried out at several temperatures up to 120 K using neutrons of incident wavelengths 2.2 \AA ($E_i = 17 \text{ meV}$) and 5.1 \AA ($E_i = 3.1 \text{ meV}$) on the time-of-flight spectrometers (IN4 and IN6) at the Institut Laue Langevin, Grenoble, France. The time-of-flight data were transformed to $S(Q, \omega)$ after correction of the data for background and

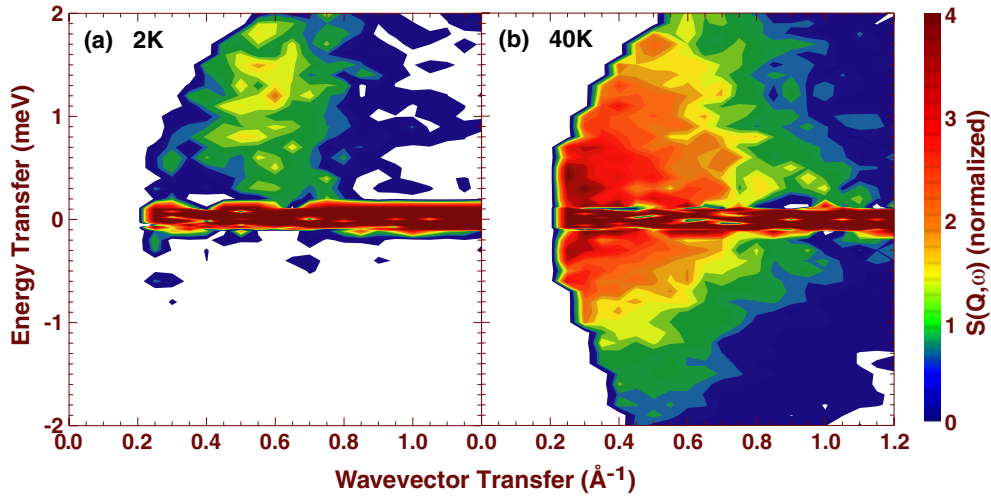


Figure 1. Two-dimensional contour plots of the normalized spectral distribution $S(Q, \omega)$ at 2 and 40 K. Note that at low temperatures the intensity is peaked on $Q = 0.6 \text{ \AA}^{-1}$, but shifts rapidly to low Q and ω as the temperature is increased to 10 K and higher.

normalization with respect to a standard vanadium sample measured using the same experiment configuration. The data were also converted to the constant Q format for discrete Q values for further analysis. Measurements under the same conditions were also performed on a LiTi_2O_4 sample as a reference for estimating the non-magnetic contributions. These contributions were then subtracted out.

3. Results and discussion

In figure 1 the contour plots of the low energy data, $S(Q, \omega)$ ($\lambda = 5.1 \text{ \AA}$, $E_i = 3.1 \text{ meV}$), at 2 and 40 K demonstrate the marked evolution of the magnetic response towards low Q vectors and energies ω as the temperature increases. Figure 2 shows the data at the same two temperatures as well as at 10 K plotted as conventional constant Q spectra for Q vectors increasing from 0.35 \AA^{-1} , the lowest Q vector accessed, covering a usefully large energy range. In the higher neutron energy experiment ($\lambda = 2.2 \text{ \AA}$, $E_i = 17 \text{ meV}$) the available angular range of detectors permitted us to obtain data only above 0.7 \AA^{-1} where this spectral evolution towards low energies and low Q is less evident.

In metallic systems, such as very dilute alloys or rare-earth systems with very weak inter-site couplings, the paramagnetic spectral response shows, in general, a dissipative, relaxational form, namely $\sim \exp(-t/\tau_0)$, due to coupling with the conduction electrons. This Fourier transforms to the Lorentzian spectral distribution. Previous neutron scattering experiments on LiV_2O_4 were both analysed using such a single-pole approximation i.e. a single Lorentzian spectral distribution. We find, however, that the magnetic response from LiV_2O_4 is more complex which is perhaps not surprising in view of its very complex character.

If we consider the magnetic response from spin glasses, for example, where some initial analyses were performed also using a single Lorentzian spectral component, it is now generally accepted that it should represent a broad distribution of relaxation times corresponding to a broad distribution of exchange couplings amongst the spins. It has been shown that the observed spectral function for spin glasses can be analysed in terms of a broad distribution of Lorentzian spectral components [11]. The imaginary part of the susceptibility response $\chi''(Q, \omega)$ from

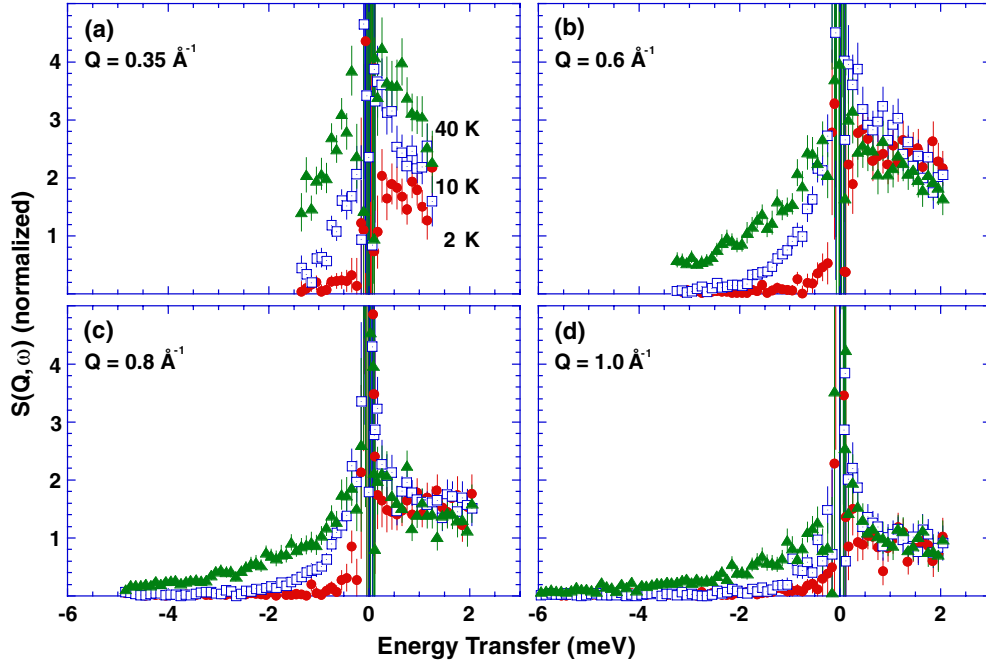


Figure 2. The normalized spectral distribution $S(Q, \omega)$ of figure 1 now plotted as a function of the energy transfer ω for several Q values at 2, 40 K as well as at 10 K. Note the marked increase in the intensity for $\omega > 0$ at the lower Q values (0.35 \AA^{-1}) compared with the higher Q values. The increase in intensity on the neutron energy gain side ($\omega < 0$) seen for all Q values is due mostly to the increasing population factor (detailed balance).

spin glasses can be expressed as

$$\chi''(Q, \omega) = \omega \sum_i \frac{\chi_i^Q \Gamma_i^Q}{[(\Gamma_i^Q)^2 + \omega^2]} \quad (1)$$

where χ_i^Q is the i th component of static ($\omega = 0$) susceptibility and Γ_i^Q is the half-width of the Lorentzian line-shape.

Also, in a uniform paramagnetic metallic lattice with spins on equivalent sites one rarely observes a magnetic response that can be analysed within a single-pole approximation due, presumably, to contributions from the various near-neighbour, next-near-neighbour and other exchange interactions. In the case of LiV_2O_4 the situation is expected to be more complicated due to the fact that the average d electron occupancy at the vanadium site (B site) is fractional with, on average, 1.5 d electrons/V. The on-site correlations of the itinerant fraction (0.5 d electrons/V site) with the localized d electron on each V site could result in rapid moment fluctuations which would also contribute to the spectral response with components of fairly broad spectral extent.

These considerations aside, the simple observation of the marked evolution of the scattering towards low energies and low Q vectors ($Q \rightarrow 0$) with increasing temperatures above 2 K also suggests that a single spectral component alone could not adequately represent the observed scattering over a wide energy range. While our data at low temperatures over the limited energy range accessed (in neutron energy loss spectroscopy—that is $\omega > 0$) can be fitted to a single Lorentzian spectral form, the fits appear distinctly poor at higher temperatures

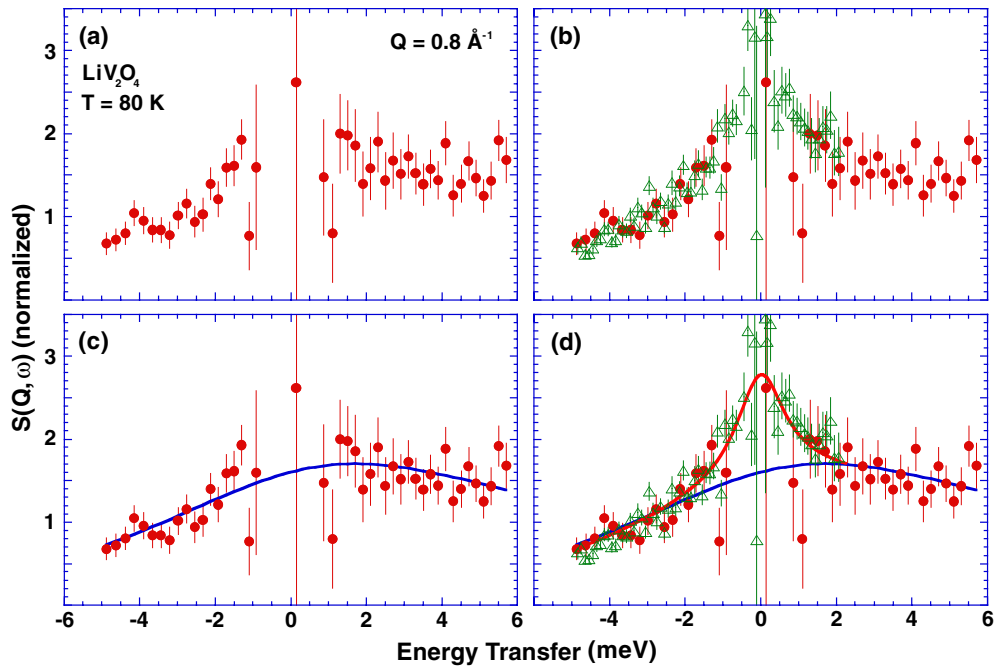


Figure 3. $S(Q, \omega)$ as a function of the energy transfer ω at 80 K for $Q = 0.8 \text{ \AA}^{-1}$. (a) shows data obtained using neutrons of incident wavelength 2.2 \AA (17 meV) and in (b) we show the same data superposed on those obtained using 5.1 \AA (3 meV) neutrons. A single-pole (Lorentzian) fit to the 2.2 \AA data is shown in (c) while the fit using two (Lorentzian) spectral components is shown in (d).

where a progressively larger energy range is accessed in neutron energy gain ($\omega < 0$), in addition to the energy range covered on the neutron energy loss side ($\omega > 0$).

We illustrate this with reference to figure 3 where in figure 3(a) we show the 80 K data at 0.8 \AA^{-1} obtained with 2.2 \AA neutrons. At this temperature and wavevector (which is close to the ‘critical’ wavevector $Q \sim 0.6 \text{ \AA}^{-1}$) an energy region of $\sim \pm 6 \text{ meV}$, symmetric about zero energy, could be accessed with neutrons of this incident energy (17 meV). In figure 3(b) we have superposed the data obtained with 5.1 \AA neutrons at the same temperature and Q . While the energy range covered in neutron energy gain ($\omega < 0$) is very similar for both data sets at this Q value, the spectrum extends to 2 meV only on the neutron energy loss side ($\omega > 0$) in the measurements performed with 5.1 \AA neutrons. The central energy region (around zero energy transfer) is dominated by resolution-limited elastic incoherent scattering from the sample typically around 3%–6% of the incident energy. This low energy region is investigated in better detail with lower incident energy neutrons (5.1 \AA), and hence a correspondingly better energy resolution. In figure 3(c) we show the best fit to the 2.2 \AA data using a single Lorentzian spectral component where the central region, $\pm 1 \text{ meV}$ (containing the non-magnetic incoherent nuclear scattering) is excluded from the fit. It is evident from the figure that a single Lorentzian spectral function does not adequately describe the observed scattering. In figure 3(d) we show the best fit obtained using two Lorentzian spectral components that are found to have significantly different widths. Evidently, they give a better representation of the data over the energy range covered. While additional spectral components cannot be ruled out, the minimum number of *sufficiently distinct* spectral components required to account satisfactorily for the data at finite temperatures *over the energy range investigated here* appears to be two. We note that

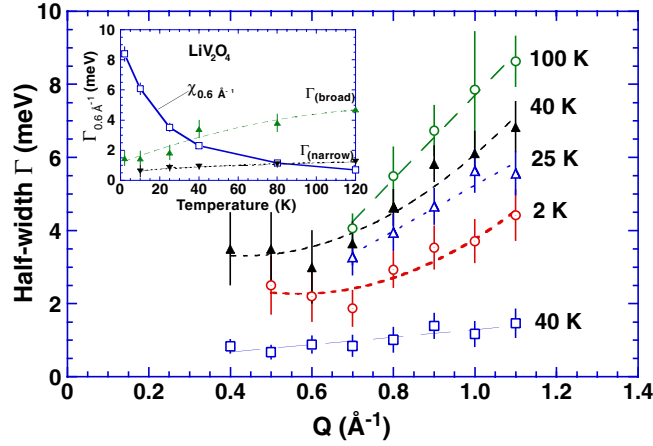


Figure 4. The observed Q dependence of the half-width Γ of the broad spectral component at a few representative temperatures. The Q variation of the narrow spectral component is also shown for the 40 K data set. The inset shows the temperature variation of both the broad and the narrow spectral components at the ‘critical’ wavevector $Q = 0.6 \text{ \AA}^{-1}$, as well as the (total) susceptibility $\chi (0.6 \text{ \AA}^{-1})$.

the energy range covered here, although larger than in previous studies, is still rather restricted (due to neutron kinematics within the available angular range of detectors and incident energies used) and does not permit us to discern possible high energy contributions due to itinerant d electrons or relatively strong spin–spin interactions.

In figure 4 we present the results for the spectral widths plotted as function of Q for several temperatures. The low temperature data at 2 K were fitted to a single Lorentzian spectral function while the higher temperature data at 10 K and above were fitted using two Lorentzian components. The Q variation for both components is shown for the 40 K data. It is interesting that the spectral width of the narrow component increases slowly with Q while that for the broad component shows a shallow ‘minimum’ or a change of slope in the region of the critical wavevector $Q \sim 0.6 \text{ \AA}^{-1}$. The temperature variations of the widths of the two spectral components at $Q = 0.6 \text{ \AA}^{-1}$ as well as the susceptibility $\chi (0.6 \text{ \AA}^{-1})$ are shown in the inset. The susceptibility at this $Q (0.6 \text{ \AA}^{-1})$ appears to be increasing slowly with decreasing T down to low temperatures while the bulk susceptibility ($Q \rightarrow 0$) shows saturation (or a broad maximum) around ~ 25 K. We remark that this low- Q region around, and below, $Q \sim 0.6 \text{ \AA}^{-1}$ could not be well investigated here since the accessed energy range is small and becomes progressively smaller with decreasing Q , as seen from figures 1 and 2. This low Q region is, in general, rather difficult to access in measurements with neutrons. However, a better coverage of the ‘ Q – ω range’ compared with the present data should be possible with spectrometers permitting high energy resolution at moderately high neutron energies and very low scattering angles. Such measurements are necessary to enable a proper extrapolation of the neutron data to $Q \rightarrow 0$ and thence a comparison with the $Q = 0$ magnetic properties, such as the bulk susceptibility. For the present we focus mainly on the higher Q data where the energy range covered is just adequate to enable us to make a connection with the specific heat of LiV_2O_4 . We show below that the latter can be well accounted for by the observed paramagnetic fluctuations, i.e. the spin degrees of freedom.

The specific heat $C = dE/dT$ can be evaluated via the expression for the mean free energy $E = \int f(E, T)N(E) dE$ with $f(E, T) = [1 - \exp(-\omega/T)]^{-1}$, for a spin fluctuation system, and $N(E)$ is the density of states. We assume that the paramagnetic spectrum is well

represented by strongly correlated (i.e. Q -dependent) Lorentzian spectral components; hence,

$$N(E) = n(\omega) = \frac{\nu}{\pi} \sum_i \sum_Q \left[\frac{\Gamma_i^Q}{(\Gamma_i^Q)^2 + \omega^2} \right]. \quad (2)$$

The factor ν represents the spatial degrees of freedom. Although the localized moments on V are quite plausibly $S = 1/2$ spins, we still take $\nu = 3$ since the observed paramagnetic fluctuations involve groups of correlated spins. The integral can be evaluated for $T \rightarrow 0$ to yield

$$\frac{C}{T} = \frac{\pi k_B^2}{T} \sum_i [\Gamma_i^Q]_{\text{av}}^{-1}. \quad (3)$$

Using this expression we obtain a mean spectral width $\sum_i [\Gamma_i^Q]_{\text{av}}^{-1}$ of ~ 5.3 meV for $\gamma = 0.42 \text{ J mol}^{-1} \text{ K}^{-2}$. This is close to the observed value $\Gamma_1^Q \sim 5$ meV at $\sim 1.2 \text{ \AA}^{-1}$ obtained from the single-component fit to the low T data. Although a Q average over the Brillouin zone (BZ) would yield a mean value smaller by some $\sim 30\%$, we note that the single-component fit itself represents a lower estimate for $\sum_i [\Gamma_i^Q]_{\text{av}}^{-1}$.

4. Conclusion

In conclusion, we have shown that a description of the spin dynamics in terms of two spectral components, a low energy component with weakly Q -dependent scattering peaked in the forward direction and a broader component showing spin correlations peaked at a finite Q vector at low temperatures, gives a reasonably good description of the observed paramagnetic spectral response from LiV_2O_4 over the energy range covered in this study. It is interesting to consider the possibility that the observed evolution of ferromagnetic-like correlations may be associated with the role of Hund's rule coupling between the localized d moment and the conduction d electrons [12]. Another possible interpretation of the spectral response could be in terms of two dominant exchange interactions between the localized d electrons on the V sites. In such a case it would appear that the role of, or the spectral response due to, the conduction electrons (i.e. itinerant d electrons) remains non-elucidated. Clearly further high resolution measurements at higher incident energies and down to lower Q values would help to shed further light on the spin dynamics of LiV_2O_4 . Finally, an interesting result from the present investigation is that spin degrees of freedom give a reasonably good account of the large specific coefficient γ of LiV_2O_4 .

References

- [1] Kondo S *et al* 1997 *Phys. Rev. Lett.* **78** 3729
- [2] Fujiwara N, Yasuoka H and Ueda Y 1998 *Phys. Rev. B* **57** 3539
- [3] Hayakawa T, Shimada D and Tsuda N 1989 *J. Phys. Soc. Japan* **58** 2867
- [4] Fulde P, Yaresko A N, Zvyagin A A and Grin Y 2001 *Europhys. Lett.* **54** 779
- [5] Anisimov V I, Korotin M A, Zöfl M, Pruschke T, Le Hur K and Rice T M 1999 *Phys. Rev. Lett.* **83** 364 and references therein
- [6] Urano C, Nohara M, Kondo S, Sakai F, Takagi H, Shiraki T and Okubo T 2000 *Phys. Rev. Lett.* **85** 1052
- [7] Fujiwara N, Yasuoka H and Ueda Y 1998 *Phys. Rev. B* **57** 3539
- [8] Johnston D C 2000 *Physica B* **281/282** 21
- [9] Krimmel A, Loidl A, Klemm M, Horn S and Schober H 1999 *Phys. Rev. Lett.* **82** 2919
- [10] Lee S-H, Qiu Y, Broholm C, Ueda Y and Rush J J 2001 *Phys. Rev. Lett.* **86** 5554
- [11] Murani A P 1981 *J. Magn. Magn. Mater.* **22** 271
- [12] Burdin S, Lacroix C and Perkins N B 2004 *J. Phys.: Condens. Matter* **16** S621